

Important Notice to Authors

No further publication processing will occur until we receive your response to this proof.

Attached is a PDF proof of your forthcoming article in *Physical Review Letters*. The article accession code is LZ15980.

Your paper will be in the following section of the journal: LETTERS — Atomic, Molecular, and Optical Physics

Please note that as part of the production process, APS converts all articles, regardless of their original source, into standardized XML that in turn is used to create the PDF and online versions of the article as well as to populate third-party systems such as Portico, Crossref, and Web of Science. We share our authors' high expectations for the fidelity of the conversion into XML and for the accuracy and appearance of the final, formatted PDF. This process works exceptionally well for the vast majority of articles; however, please check carefully all key elements of your PDF proof, particularly any equations or tables.

Figures submitted electronically as separate files containing color appear in color in the online journal.

However, all figures will appear as grayscale images in the print journal unless the color figure charges have been paid in advance, in accordance with our policy for color in print (<https://journals.aps.org/authors/color-figures-print>).

Specific Questions and Comments to Address for This Paper

The numbered items below correspond to numbers in the margin of the proof pages pinpointing the source of the question and/or comment. The numbers will be removed from the margins prior to publication.

- 1 Is there a collaboration name that should be added with the author list?
- 2 Please verify authors, affiliations, and all cross-referencing.
- 3 Slashes are generally used only for mathematical and chemical expressions in this journal because they are often ambiguous in text. Please note the changes to replace slashes with the appropriate word or character throughout. If these are not correct, please explain.
- 4 Please verify the change to 30-fs here. Is this correct?
- 5 Please verify the degree symbol added with 14 in the expression for 2 theta. Is this correct?
- 6 Please verify the change to “TOF-type” here. Is this correct?
- 7 Please verify the change to “several hundred femtoseconds” here. Is this correct?
- 8 Please verify the change to “a few tens of percent”. Is this correct?
- 9 What is a.u. used in Fig. 3?
- 10 Please verify the change to “spot intensity based model is added”. Is this correct?
- 11 Please verify the change to “hereafter defined as shrinkage.” Is this correct?
- 12 Please verify the change to “with a speed compatible with the plasma speed of sound”. Is this correct?
- 13 Please verify all changes made in the Acknowledgments section.
- 14 Please review the funding information section of the proof’s cover letter and respond as appropriate. We must receive confirmation that the funding agencies have been properly identified before the article can publish.
- 15 This query was generated by an automatic reference checking system. Reference [17] could not be located in the databases used by the system. While the reference may be correct, we ask that you check it so we can provide as many links to the referenced articles as possible.
- 16 NOTE: External links, which appear as blue text in the reference section, are created for any reference where a Digital Object Identifier (DOI) can be found. Please confirm that the links created in this PDF proof, which can be checked by clicking on the blue text, direct the reader to the correct references online. If there is an error, correct the information in the reference or


supply the correct DOI for the reference. If no correction can be made or the correct DOI cannot be supplied, the link will be removed.

- 17** Please provide a brief description of the Supplemental Material to be included in the reference to this material. Note url for supplemental reference will be added at the time of publication.

Titles in References

The editors now encourage insertion of article titles in references to journal articles and e-prints. This format is optional, but if chosen, authors should provide titles for *all* eligible references. If article titles remain missing from eligible references, the production team will remove the existing titles at final proof stage.

ORCIDs

Please follow any ORCID links () after the authors' names and verify that they point to the appropriate record for each author.

Funding Information

Information about an article's funding sources is now submitted to Crossref to help you comply with current or future funding agency mandates. Crossref's Open Funder Registry (<https://www.crossref.org/services/funder-registry/>) is the definitive registry of funding agencies. Please ensure that your acknowledgments include all sources of funding for your article following any requirements of your funding sources. Where possible, please include grant and award ids. Please carefully check the following funder information we have already extracted from your article and ensure its accuracy and completeness:

- Ministry of Education, Culture, Sports, Science and Technology, FundRef ID <http://dx.doi.org/10.13039/501100001700> (Japan/JP)
- Japan Society for the Promotion of Science, FundRef ID <http://dx.doi.org/10.13039/501100001691> (Japan/JP)
- Consiglio Nazionale delle Ricerche, FundRef ID <http://dx.doi.org/10.13039/501100004462> (Repubblica Italiana/IT)
- Japan-Italy Research Cooperative Program
- U.S. Department of Energy, FundRef ID <http://dx.doi.org/10.13039/100000015> (United States/US)
- Office of Basic Energy Sciences
- Argonne National Laboratory, FundRef ID <http://dx.doi.org/10.13039/100006224> (United States/US)
- UChicago Argonne
- Ministero dell'Istruzione, dell'Università e della Ricerca, FundRef ID <http://dx.doi.org/10.13039/501100003407> (Repubblica Italiana/IT)

Other Items to Check

- Please note that the original manuscript has been converted to XML prior to the creation of the PDF proof, as described above. Please carefully check all key elements of the paper, particularly the equations and tabular data.
- Title: Please check; be mindful that the title may have been changed during the peer-review process.
- Author list: Please make sure all authors are presented, in the appropriate order, and that all names are spelled correctly.
- Please make sure you have inserted a byline footnote containing the email address for the corresponding author, if desired. Please note that this is not inserted automatically by this journal.
- Affiliations: Please check to be sure the institution names are spelled correctly and attributed to the appropriate author(s).
- Receipt date: Please confirm accuracy.
- Acknowledgments: Please be sure to appropriately acknowledge all funding sources.
- References: Please check to ensure that titles are given as appropriate.

- Hyphenation: Please note hyphens may have been inserted in word pairs that function as adjectives when they occur before a noun, as in “x-ray diffraction,” “4-mm-long gas cell,” and “*R*-matrix theory.” However, hyphens are deleted from word pairs when they are not used as adjectives before nouns, as in “emission by x rays,” “was 4 mm in length,” and “the *R* matrix is tested.”
Note also that Physical Review follows U.S. English guidelines in that hyphens are not used after prefixes or before suffixes: superresolution, quasiequilibrium, nanoprecipitates, resonancelike, clockwise.
- Please check that your figures are accurate and sized properly. Make sure all labeling is sufficiently legible. Figure quality in this proof is representative of the quality to be used in the online journal. To achieve manageable file size for online delivery, some compression and downsampling of figures may have occurred. Fine details may have become somewhat fuzzy, especially in color figures. The print journal uses files of higher resolution and therefore details may be sharper in print. Figures to be published in color online will appear in color on these proofs if viewed on a color monitor or printed on a color printer.
- Overall, please proofread the entire *formatted* article very carefully. The redlined PDF should be used as a guide to see changes that were made during copyediting. However, note that some changes to math and/or layout may not be indicated.

Ways to Respond

- **Web:** If you accessed this proof online, follow the instructions on the web page to submit corrections.
- **Email:** Send corrections to aps-robot@luminad.com. Include the accession code LZ15980 in the subject line.
- **Fax:** Return this proof with corrections to +1.855.808.3897.

If You Need to Call Us

You may leave a voicemail message at +1.855.808.3897. Please reference the accession code and the first author of your article in your voicemail message. We will respond to you via email.

Ultrafast Structural Dynamics of Nanoparticles in Intense Laser Fields

Toshiyuki Nishiyama,^{1,2} Yoshiaki Kumagai,³ Akinobu Niozu,^{1,2} Hironobu Fukuzawa,^{2,3} Koji Motomura,³ Max Bucher,⁴ Yuta Ito,³ Tsukasa Takanashi,³ Kazuki Asa,^{1,2} Yuhiro Sato,^{1,2} Daehyun You,³ Yiwen Li,³ Taishi Ono,³ Edwin Kukk,⁵ Catalin Miron,^{6,7} Liviu Neagu,^{7,8} Carlo Callegari,⁹ Michele Di Fraia,⁹ Giorgio Rossi,¹⁰ Davide E. Galli,¹⁰ Tommaso Pincelli,^{10,11} Alessandro Colombo,¹⁰ Takashi Kameshima,¹² Yasumasa Joti,¹² Takaki Hatsui,² Shigeki Owada,² Tetsuo Katayama,¹² Tadashi Togashi,¹² Kensuke Tono,¹² Makina Yabashi,² Kazuhiro Matsuda,¹ Christoph Bostedt,^{4,13,14,*} Kiyonobu Nagaya,^{1,2,†} and Kiyoshi Ueda^{2,3,‡}

¹*Division of Physics and Astronomy, Kyoto University, Kyoto 606-8501, Japan*

²*RIKEN SPring-8 Center, Sayo, Hyogo 679-5148, Japan*

³*Institute of Multidisciplinary Research for Advanced Materials, Tohoku University, Sendai 980-8577, Japan*

⁴*Chemical Sciences and Engineering Division, Argonne National Laboratory, 9700 South Cass Avenue, Argonne, Illinois 60439, USA*

⁵*Department of Physics and Astronomy, University of Turku, 20014 Turku, Finland*

⁶*LIDYL, CEA, CNRS, Université Paris-Saclay, CEA Saclay, 91191 Gif-sur-Yvette, France*

⁷*Extreme Light Infrastructure-Nuclear Physics (ELI-NP), “Horia Hulubei” National Institute for Physics and Nuclear Engineering, 30 Reactorului Street, RO-077125 Măgurele, Jud. Ilfov, Romania*

⁸*National Institute for Laser, Plasma and Radiation Physics, 409 Atomistilor PO Box MG-36, 077125 Măgurele, Jud. Ilfov, Romania*

⁹*Elettra-Sincrotrone Trieste, 34149 Basovizza, Trieste, Italy*

¹⁰*Department of Physics, Università degli Studi di Milano, Via Celoria 16—20133 Milano, Italy*

¹¹*Fritz Haber Institute of the Max Planck Society, Faradayweg 4-6, 14195 Berlin, Germany*

¹²*Japan Synchrotron Radiation Research Institute (JASRI), Sayo, Hyogo 679-5198, Japan*

¹³*Paul-Scherrer Institute, CH-5232 Villigen PSI, Switzerland*

¹⁴*LUXS Laboratory for Ultrafast X-ray Sciences, Institute of Chemical Sciences and Engineering, École Polytechnique Fédérale de Lausanne (EPFL), CH-1015 Lausanne, Switzerland*

(Received 20 December 2018; revised manuscript received 22 April 2019)

1 Femtosecond laser pulses have opened new frontiers for the study of ultrafast phase transitions and
2 nonequilibrium states of matter. In this Letter, we report on structural dynamics in atomic clusters pumped
 with intense near-infrared (NIR) pulses into a nanoplasma state. Employing wide-angle scattering with
 intense femtosecond x-ray pulses from a free-electron laser source, we find that highly excited xenon
 nanoparticles retain their crystalline bulk structure and density in the inner core long after the driving NIR
 pulse. The observed emergence of structural disorder in the nanoplasma is consistent with a propagation
 from the surface to the inner core of the clusters.

DOI:

When matter is irradiated by an intense femtosecond laser pulse, the rapid energy deposition can trigger new and diverse phenomena including nonthermal melting [1,2], bond hardening [3], or the creation of dense electron-hole plasma [4]. For all of these ultrafast phase transitions, drastic structural changes are expected to occur, and understanding the competing timescales of the driving mechanisms of excitation and deexcitation in these highly excited systems is of fundamental interest.

Atomic clusters have become a test bed for nonlinear light-matter interaction studies [5]. A rare-gas cluster exposed to an intense near-infrared (NIR) laser pulse becomes highly ionized, by multiphoton absorption, and can evolve into a nanoscale plasma, called nanoplasma [6,7], which expands quickly just after formation due to Coulombic or hydrodynamic forces [8]. So far, virtually all information about nanoplasma has been deduced from ion and electron time-of-flight (TOF) measurements. But now, intense femtosecond

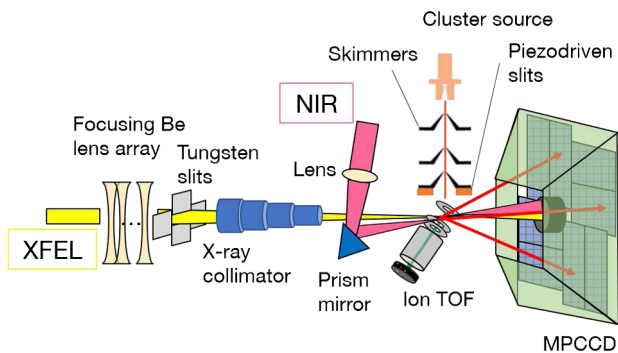
x-ray pulses from novel free-electron laser sources allow imaging the structural dynamics of highly excited systems down to a few tens of nanometers in size with unprecedented spatial and temporal resolution. Recently, structural changes of laser-driven clusters were studied with time-resolved single-shot imaging methods, which give information on temporal evolution of cluster shape [9]. Using the small-angle x-ray scattering information, the authors reported ultrafast and nonuniform morphology changes of giant xenon (Xe) clusters in agreement with calculations on hydrogen clusters [10]. These studies gave insight into changes of the averaged density profile in nanoplasma formation induced by intense laser field, showing that the nanoplasma expansion is initiated by rapid surface softening. However, the question on the local atomic order in the cluster core during nanoplasma formation remains.

Following the local atomic order with Bragg scattering experiments has been pivotal to understanding ultrafast

light-induced phase transitions [1–4,11–13]. For nano-
 plasma, a recent time-resolved x-ray pump–x-ray probe
 wide-angle x-ray scattering (WAXS) study observed Bragg
 reflections shifting to larger momentum transfer and, thus,
 suggesting lattice contraction of Xe nanocrystals induced
 within femtoseconds by the first x-ray free-electron laser
 (XFEL) pulse [12]. The lattice contraction was attributed to
 the sudden change in the potential energy landscape upon
 core-level ionization and decay. Intense optical fields,
 however, dominantly couple to the valence electrons and
 therefore they are anticipated to induce different dynamics.

In this Letter, we report on ultrafast Bragg scattering
 experiments on Xe clusters in intense NIR laser fields. We
 find that the lattice order survives significantly longer than
 the 30-fs driving NIR pulse. From the detailed analysis of
 the Bragg reflections we can deduce that the crystalline
 core radius shrinks while maintaining the initial crystalline
 structure. Comparing the nanoplasma core data to the
 plasma parameters indicates that the observed dynamics are
 governed by plasma speed of sound.

Our NIR pump–x-ray probe experiments were carried out
 at the SPring-8 Angstrom Compact Free Electron Laser
 (SACLA) [14]. A sketch of the experiment is shown in Fig. 1
 and, in short, a jet of free Xe clusters was irradiated by a
 single NIR laser pulse followed, at selected delays, by single
 XFEL pulses. The cluster jet was generated by an adiabatic
 expansion of Xe gas through a convergent-divergent nozzle
 with a 200- μm diameter and a half angle of 4° at a stagnation
 pressure of 30 bar and nozzle temperature of 290 K. The
 average cluster size was estimated to be around 1×10^7
 atoms/cluster by Hagena’s scaling law [15]. The cluster jet
 passed through two skimmers (0.5 and 2 mm) and was finally
 tailored with piezodriven slits so that its size in the direction
 of the laser pulses was smaller than the Rayleigh length of the
 laser pulses.



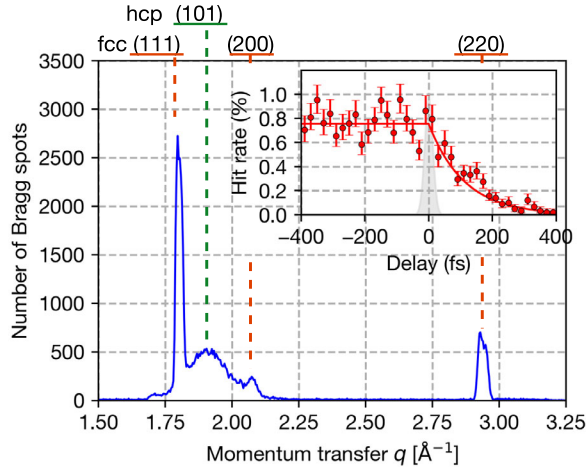
F1:1 FIG. 1. Experimental setup. The x-ray pulses are focused with
 F1:2 Be lenses [16] onto a multiple skimmed jet of Xe clusters and
 F1:3 their WAXS patterns are recorded with a MPCCD detector. NIR
 F1:4 pulses are overlapped in the interaction region in a close to
 F1:5 collinear geometry with a prism mirror and pump the clusters into
 F1:6 a nanoplasma state. Ion TOF spectroscopy is used to determine
 F1:7 the temporal overlap between the two lasers.

The NIR laser pulses with a wavelength of 800 nm and
 pulse length of 30 fs were focused with a single plano-
 convex lens ($f = 500$ mm) and overlapped with the XFEL
 pulses with a prism mirror at an angle of 3° . A spot size of
 $(4 \times 10^1) \times (4 \times 10^1) \mu\text{m}^2$ was given for that of the NIR
 laser at the reaction point. The pulse energy of the NIR laser
 was adjusted to get an intensity of 4×10^{16} W/cm 2 . The
 XFEL pulses had a wavelength (λ) of 1.1 Å and pulse
 duration of 10 fs (FWHM). They were focused with Be
 lenses to a spot size of $1.4 \times 1.6 \mu\text{m}^2$, significantly smaller
 than the NIR focus, resulting in an intensity of
 4×10^{17} W/cm 2 . Spatial and temporal overlap between
 XFEL and NIR pulses was determined through measuring
 TOF spectra of the clusters. The delay time of the NIR
 pulse relative to the XFEL pulse was controlled by an
 optical delay system in the range of -500 to $+2000$ fs. The
 positive delay corresponds to a NIR laser arriving early and
 a XFEL late. The temporal jitter between the arrival time of
 the XFEL and NIR pulses was measured with the arrival
 time monitor with 20-fs precision [17].

The scattered x-ray photons were recorded with a
 multiport charge-coupled device (MPCCD) octal sensor
 [18] installed 100 mm downstream from the reaction point.
 An Al-coated stainless-steel baffle was installed to reduce
 stray light and fluorescence from the chamber. The detector
 was also protected with a Kapton foil of 75- μm thickness.
 The NIR and x-ray pulses were dumped into a three-layer
 beam stop consisting of C, Al, and W sandwich structure.
 In our setup the observable range of momentum transfer,
 $q = (4\pi/\lambda) \sin \theta$, was 1.4–3.4 Å $^{-1}$, corresponding to $2\theta =$
 14° – 35° in scattering angle. Xe ions were detected by the
 TOF-type ion spectrometer [19].

In a first step, static WAXS information was recorded in
 order to confirm the crystallinity of the nanoparticles. On
 average we could observe a few Bragg spots for each shot
 on the detector, indicating that we produced a dense target
 of clusters in the x-ray and NIR focus. Figure 2 shows the
 radial average of Bragg spots observed in 638869 shots.
 The radial profile has peaks at the positions of reflections
 from (111), (200), and (220) planes of face-centered cubic
 (fcc) lattice. Observed fcc structure of Xe clusters agrees
 well with the structure and lattice constant of bulk Xe [20].
 The spots corresponding to hcp (101) Bragg reflection were
 also observed, and these can be attributed to Xe crystals
 with randomly stacked close-packed structure [21]. This
 means that the obtained data include both nearly perfect fcc
 crystals and nearly randomly stacked crystals. However, the
 difference of stacking has no effects on the profiles of
 intense Bragg spots that appear at the fcc (111) reflection
 region ($q \sim 1.79$ Å $^{-1}$) [21]. Considering the above facts,
 the present analysis focuses on the spots observed at
 $q \sim 1.79$ Å $^{-1}$.

In the inset of Fig. 2 the hit rate, defined as the number of
 detected Bragg spots normalized to the number of XFEL
 shots, for fcc (111) is plotted as a function of delay time.



F2:1 FIG. 2. Radial average of the observed Bragg spots for
 F2:2 unpumped clusters. Bragg reflections at the positions of (111),
 F2:3 (200), and (220) planes of the fcc lattice are detected. The inset
 F2:4 shows the decrease in hit rate as a function of the delay time for
 F2:5 pumped clusters. The data points shown in the inset were derived
 F2:6 by averaging the whole data in each delay point.

160 The decrease of the hit rate indicates the progressive
 161 reduction of coherent diffraction during the nanoplasma
 162 formation, but it is noteworthy that the fcc crystal structure
 163 **7** of Xe clusters survives for several hundred femtoseconds
 164 after laser irradiation. We also point out that the momentum
 165 transfer of (111) Bragg reflection spots did not change
 166 within the experimental error ($\pm 0.01 \text{ \AA}^{-1}$). This observa-
 167 tion suggests that the change of the lattice constant of the
 168 Xe fcc crystal is negligible. A recent time-resolved x-ray
 169 pump-x-ray probe wide-angle x-ray scattering observed
 170 Bragg reflections shifting to larger momentum transfer in
 171 the excited nanoparticles, indicating the occurrence of
 172 lattice contraction of Xe nanocrystals within femtoseconds
 173 from the 10-fs hard x-ray pump pulse [12]. The lattice
 174 contraction was explained as a consequence of the sudden
 175 change in the potential energy landscape upon core-level
 176 ionization and decay. Our present results, as obtained with
 177 an intense optical pump field, show a different nanoparticle
 178 behavior: diffracting volume reduction, but no lattice
 179 contraction. The largest excitation cross sections for intense
 180 NIR pulses are valence excitation and inverse bremsstrahlung
 181 heating [6], while x rays excite primarily core
 182 electrons. We therefore speculate that the density profile
 183 of the nanoparticle excitation is quite different in the two
 184 experiments and that the observed structural evolution of
 185 the nanoparticles does reflect such different excitation
 186 regimes. At present we are unable to make a fully qualified
 187 statement in this matter, which will need theoretical support
 188 describing the complex and correlated electron and nuclear
 189 dynamics.

190 Before delving into a detailed analysis of the Bragg
 191 spots, the signal generation shall be briefly discussed.
 192 Supersonic jet expansion always leads to a distribution

193 in cluster sizes [15]. Further, the x-ray scattering signal is
 194 convoluted with the focal volume intensity distribution
 195 [22]. In order to create a reliable dataset we therefore only
 196 considered the 5% most intense signals at each delay point,
 197 i.e., only the signal from the largest clusters in the hottest
 198 part of the x-ray focal volume.

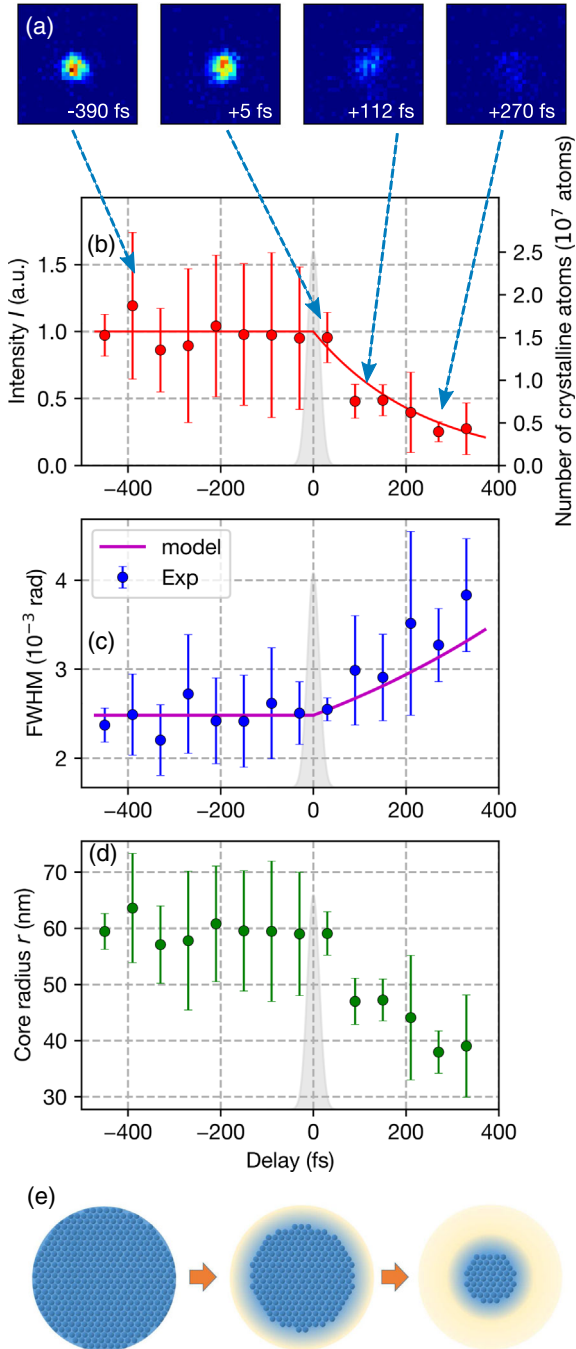
199 To obtain information on the local structural changes in Xe
 200 clusters, we carried out a profile analysis of Bragg spots.
 201 According to the x-ray scattering theory, the Bragg spot
 202 intensity is related to the crystal volume, the photon density,
 203 and the random displacement of atoms in crystal (the Debye-
 204 Waller factor). The spot width is related to the particle size
 205 and strain of crystal. We estimated the intensity, which is the
 206 product of the area and the height of the Bragg spot, and width
 207 of each Bragg spot by fitting with a 2D Gaussian function. In
 208 Fig. 3(a) we show the characteristic spots from fcc (111)
 209 reflection at various delay times. Figures 3(b) and 3(c) show
 210 the temporal evolution of fitted intensity and width of the fcc
 211 (111) Bragg spots. The data show that the intensity of Bragg
 212 spots was weakened upon NIR irradiation [Fig. 3(b)], which
 213 is consistent with the decrease of the hit rate. At the same time,
 214 the spot width increased [Fig. 3(c)], and the increase reached a
 215 few tens of percent. **8**

216 The simultaneous decrease in intensity and increase in
 217 Bragg spot width indicates that the crystal volume
 218 decreases [23], or in other words, a nonuniform process
 219 for crystal disordering. A uniform random displacement of
 220 the atoms in the crystal, represented with the Debye-Waller
 221 approximation, would not affect the spot width. To sub-
 222 stantiate this interpretation we performed Bragg scattering
 223 calculations on a simplified model (see the Supplemental
 224 Material for details [24]). In our model we assumed three
 225 principal disordering mechanisms: a random disorder, a
 226 core disorder, and a surface disorder. The results show that
 227 the surface disorder is in best agreement with the exper-
 228 imental observations and our interpretation of the Debye-
 229 Waller factor.

230 For further insight into the NIR-induced dynamics we
 231 performed a consistency check of the spot intensity and
 232 spot width data. In a first step, we started with a simple
 233 model assuming that the decrease of the spot intensity is
 234 proportional to the crystal volume and the time-dependent
 235 signal is reflecting the volume decrease. For spherical fcc
 236 Xe clusters, the crystal radius is then related to the spot
 237 intensity as follows:

$$r(t) = \begin{cases} r_0 & (t < 0) \\ r_0(I(t)/I_0)^{1/3} & (t > 0). \end{cases} \quad (1)$$

238 Here r_0 is the radius of cluster in the neutral state (60 nm),
 239 I_0 is the intensity of the Bragg spot from pristine clusters,
 240 and $r(t)$ and $I(t)$ are cluster radius and intensity of Bragg
 241 spot at the delay time t , respectively. In a second step, we
 242 calculate the resulting spot width with the Scherrer equa-
 243 tion [25], which relates the FWHM of the Bragg spot β
 244 and the size of nanoscale crystal as follows:
 245



F3:1 **9** FIG. 3. Delay dependence of profiles of Bragg spots from
 F3:2 (111) plane at the NIR power of $4 \times 10^{16} \text{ W cm}^{-2}$. (a) Characteristic
 F3:3 spot images. (b) Temporal evolution of the spot intensity
 F3:4 (markers) was fitted by an exponential function (solid red line).
 F3:5 Its decay constant was estimated to be around 200 fs. (c) Tem-
 F3:6 poral evolution of the spot width (markers) was compared with
 F3:7 surface melting model (solid magenta line). (d) The temporal
 F3:8 evolution of the core radius calculated with the experimental
 F3:9 (markers) and fitting [solid red line in (b)] data. The error bars of
 F3:10 (b)–(d) show standard deviations. (e) A scheme of cluster
 F3:11 disordering that proceeds from the surface and is consistent
 F3:12 with our experiments.

$$\beta(t) = \frac{2\lambda}{3r(t) \cos \theta}. \quad (2)$$

Here λ is the wavelength of the incident photons and θ is the Bragg angle. Note that the original formula is in terms of a generalized length scale equal to the cube root of the particle volume. The resulting Bragg peak width from this purely spot intensity based model is added to the measured spot width data in Fig. 3(c) as a solid magenta line. The modeled and measured spot width agree well, showing that the spot intensity reduction and spot width increase are correlated. The data show that the superheated clusters lose crystalline order from their surface with an ever shrinking crystalline core. The process is depicted in Fig. 3(e).

From the data and with Eq. (2) the average radius of the crystalline particle core as a function of delay can be inferred, which is shown in Fig. 3(d). The core radius of the undisturbed clusters is stable around 60 nm, but upon NIR excitation the crystalline core radius shrinks rapidly. This result is qualitatively similar to an earlier ultrafast imaging experiment which is sensitive to the envelope of the particle [9]. This previous experiment revealed that the nanoplasma expansion proceeds via a developing density gradient at the nanoparticle surface akin to nonthermal surface melting, but no information about the inner structure could be obtained. Our data show that the cluster core in the nanoplasma maintains a crystalline bulklike structure long after the NIR pump pulse is over, but the crystalline fraction is reduced over time (hereafter defined as shrinkage). From Fig. 3(d) and our model we can estimate that the core shrinks with a speed of $7 \times 10^4 \text{ m/s}$.

We can discuss our results in light of previous studies about nonlinear NIR laser—cluster interactions and nanoplasma formation [5–7]. At the early stage of laser-cluster interaction, many electrons are photoejected and the nanoscale cluster becomes positively charged. Electrons subsequently released are confined by the developing Coulomb potential, leading to the formation of a non-equilibrium nanoplasma. During the laser irradiation, electrons gain energy from the laser field and the cluster is heated via inverse bremsstrahlung processes. The nanoplasma expands into vacuum due to internal pressure of the electron gas as well as the Coulomb forces. In general, for small clusters the expansion is dictated by Coulombic interaction and for large clusters by hydrodynamic expansion [5,6,26]. In our case of very large clusters, hydrodynamic expansion with the plasma speed of sound is predicted [6,22,27].

To estimate the relevant plasma parameters, we measured the NIR laser produced ion kinetic energy distribution with a time-of-flight spectrometer in a reference measurement, similar to previous studies [6,22,27]. Fitting the ion spectra, we estimated an average charge state Z of 30 from the time-of-flight data and a resulting

299 electron density n_e of $4 \times 10^{23}/\text{cm}^3$. Using the experimen-
 300 tally determined Z and n_e in full plasma simulations with
 301 FLYCHK [28] we infer an electron temperature T_e of
 302 ~ 300 eV and an electron-ion equilibrium time τ_{e-i} [8]
 303 of ~ 350 fs. The resulting plasma speed of sound, described
 304 as $\sqrt{Zk_B T_e / M}$ (k_B is the Boltzmann constant and M is the
 305 atomic mass of Xe), is on the order of 8×10^4 m/s.

306 Most interestingly, the plasma speed of sound determines
 307 the speed of hydrodynamic expansion, and the numeric
 308 value above comes remarkably close to our measured core
 309 shrinking speed (7×10^4 m/s). While so far the interior
 310 dynamics of the nonequilibrium nanoplasmas remained
 311 elusive, our data can connect previous imaging studies on
 312 surface dynamics [9] to the dynamics in the nanoparticle
 313 core. The imaging studies [9] showed an expansion from the
 314 surface, and our results show a continuous shrinking of the
 315 crystalline volume in the core. Connecting the two datasets
 316 of surface expansion or softening (exterior dynamics) to the
 317 core shrinking and related loss of crystalline order from the
 318 surface (interior dynamics), we conclude that the disorder-
 319 ing starts on the surface and propagates to the interior
 320 with a speed compatible with the plasma speed of sound.
 321 This interpretation is compatible with ion time-of-flight
 322 studies on shell expansion in core-shell structures [29,30]
 323 and theoretical modeling of laser-driven hydrogen clusters
 324 [10]. In particular, the experimentally determined core
 325 shrinking speed is in good agreement with a theoretical
 326 study on the expansion dynamics of hydrogen nanoplasma
 327 in intense laser fields by Peltz *et al.* [10], but here we can go
 328 one step further. Our data show that even in the highly
 329 excited nonequilibrium state, the nanoplasma core retains its
 330 crystalline bulk structure and density beyond the initially
 331 driving NIR pulse and even beyond τ_{e-i} . Our interpretation
 332 is that the local disordering in nanoplasma proceeds from the
 333 surface towards the core, initially protecting the core
 334 structure and retaining the bulk lattice configuration until
 335 the surface disordering has propagated into the core. For a
 336 full understanding of the complex laser-induced dynamics,
 337 theoretical studies including the full ionization processes
 338 and plasma dynamics [10,31] will need to be performed and
 339 compared to our dataset.

340 In summary, we investigated ultrafast and atomic-scale
 341 structural changes in nanoplasma with time-resolved
 342 WAXS experiments. We revealed that the crystalline order
 343 in a Xe cluster to nanoplasma transition is maintained long
 344 after the driving laser pulse is over. Based on our diffraction
 345 data in conjunction with previous studies, we conclude that
 346 the local disordering in nanoplasma proceeds from the
 347 surface to the core with a speed compatible with the plasma
 348 speed of sound. Our findings provide new insight into the
 349 structural dynamics of highly nonequilibrium nanoplasma
 350 states, their formation, and their evolution.

351 We express our profound gratitude to our deceased
 352 colleague, Professor Makoto Yao, for his invaluable

support and help with this study. The XFEL experiments
 were performed at the BL3 of SACLA with the approval
 of the Japan Synchrotron Radiation Research Institute
 (JASRI) and the program review committee
 (2016A8057, 2016B8077). This study was supported by
 the X-ray Free Electron Laser Utilization Research Project
 and the X-ray Free Electron Laser Priority Strategy
 Program of the MEXT, the Proposal Program of SACLA
 Experimental Instruments of RIKEN, by JSPS KAKENHI
 Grant No. 15K17487, by JSPS and CNR under the Japan-
 Italy Research Cooperative Program, and by the IMRAM
 project. T.N. acknowledges support from the Research
 Program for Next Generation Young Scientists of
 “Dynamic Alliance for Open Innovation Bridging
 Human, Environment and Materials” in “Network Joint
 Research Center for Materials and Devices.” H. F., K. U.,
 and K. N. acknowledge support from the Research Program
 of “Dynamic Alliance for Open Innovation Bridging
 Human, Environment and Materials” in “Network Joint
 Research Center for Materials and Devices.” C. B. and M.
 B. acknowledge support from the U.S. Department of
 Energy, Office of Basic Energy Sciences, Division of
 Chemical Sciences, Geosciences, and Biosciences through
 Argonne National Laboratory. Argonne is a U.S.
 Department of Energy laboratory managed by UChicago
 Argonne, LLC, under Contract No. DE-AC02-
 06CH11357. G. R., D. E. G., T. P., and A. C. acknowledge
 support from NOXSS PRIN contract of MIUR, Italy. M. D.
 F. and C. C. acknowledge support from the “Japan-Italy
 Research Cooperative Program.”

* christoph.bostedt@psi.ch

† nagaya@scphys.kyoto-u.ac.jp

‡ ueda@tagen.tohoku.ac.jp

- [1] C. W. Siders, A. Cavalleri, K. Sokolowski-Tinten, C. Töth,
 T. Guo, M. Kammler, M. H. von Hoegen, K. R. Wilson,
 D. von der Linde, and C. P. J. Barty, *Science* **286**, 1340
 (1999).
 [2] G. Sciaini, M. Harb, S. G. Kruglik, T. Payer, C. T. Hebeisen,
 F. J. M. zu Heringdorf, M. Yamaguchi, M. H. von Hoegen,
 R. Ernstorfer, and R. J. D. Miller, *Nature (London)* **458**, 56
 (2009).
 [3] R. Ernstorfer, M. Harb, C. T. Hebeisen, G. Sciaini, T.
 Dartigalongue, and R. J. D. Miller, *Science* **323**, 1033
 (2009).
 [4] L. B. Fletcher, H. J. Lee, T. Döppner, E. Galtier, B. Nagler
et al., *Nat. Photonics* **9**, 274 (2015).
 [5] T. Fennel, K.-H. Meiwes-Broer, J. Tiggesbäumker, P.-G.
 Reinhard, P. M. Dinh, and E. Suraud, *Rev. Mod. Phys.* **82**,
 1793 (2010).
 [6] T. Ditmire, T. Donnelly, A. M. Rubenchik, R. W. Falcone,
 and M. D. Perry, *Phys. Rev. A* **53**, 3379 (1996).
 [7] T. Ditmire, J. W. G. Tisch, E. Springate, M. B. Mason, N.
 Hay, R. A. Smith, J. Marangos, and M. H. R. Hutchinson,
Nature (London) **386**, 54 (1997).

410	[8] V.P. Krainov and M.B. Smirnov, <i>Phys. Rep.</i> 370 , 237 (2002).	[21] P.N. Pusey, W. van Meegen, P. Bartlett, B. J. Ackerson, J. G. Rarity, and S. M. Underwood, <i>Phys. Rev. Lett.</i> 63 , 2753 (1989).	435
411			436
412	[9] T. Gorkhover, S. Schorb, R. Coffee, M. Adolph, L. Foucar <i>et al.</i> , <i>Nat. Photonics</i> 10 , 93 (2016).	[22] T. Gorkhover, M. Adolph, D. Rupp, S. Schorb, S. W. Epp <i>et al.</i> , <i>Phys. Rev. Lett.</i> 108 , 245005 (2012).	437
413			438
414	[10] C. Peltz, C. Varin, T. Brabec, and T. Fennel, <i>Phys. Rev. Lett.</i> 113 , 133401 (2014).	[23] J. Als-Nielsen and D. McMorrow, <i>Elements of Modern X-Ray Physics</i> , 2nd ed. (Wiley, New York, 2011), Sec. 5. 4.	439
415			440
416	[11] A. M. Lindenberg, J. Larsson, K. Sokolowski-Tinten, K. J. Gaffney, C. Blome <i>et al.</i> , <i>Science</i> 308 , 392 (2005).	[24] See Supplemental Material at http://link.aps.org/supplemental/10.1103/PhysRevLett.000.000000 for [brief description].	441
417			442
418	[12] K. R. Ferguson, M. Bucher, T. Gorkhover, S. Boutet, H. Fukuzawa <i>et al.</i> , <i>Sci. Adv.</i> 2 , e1500837 (2016).	[25] A. Patterson, <i>Phys. Rev.</i> 56 , 978 (1939).	443
419			17 444
420	[13] I. Inoue, Y. Inubushi, T. Sato, K. Tono, T. Katayama <i>et al.</i> , <i>Proc. Natl. Acad. Sci. U.S.A.</i> 113 , 1492 (2016).	[26] S. P. Hau-Riege, R. A. London, and A. Szoke, <i>Phys. Rev. E</i> 69 , 051906 (2004).	445
421			446
422	[14] K. Tono, T. Togashi, Y. Inubushi, T. Sato, T. Katayama <i>et al.</i> , <i>New J. Phys.</i> 15 , 083035 (2013).	[27] D. D. Hickstein, F. Dollar, J. A. Gaffney, M. E. Foord, G. M. Petrov <i>et al.</i> , <i>Phys. Rev. Lett.</i> 112 , 115004 (2014).	447
423			448
424	[15] O. F. Hagen, <i>Rev. Sci. Instrum.</i> 63 , 2374 (1992).	[28] H. K. Chung, M. H. Chen, W. L. Morgan, Y. Ralchenko, and R. Lee, <i>High Energy Density Phys.</i> 1 , 3 (2005).	449
425			450
426	[16] T. Katayama, T. Hirano, Y. Morioka, Y. Sano, T. Osaka, S. Owada, T. Togashi, and M. Yabashi, <i>J. Synchrotron Radiat.</i> 26 , 333 (2019).	[29] M. Hoener, C. Bostedt, T. Thomas, L. Landt, E. Eremina, H. Wabnitz, T. Laarmann, R. Treusch, A. R. B. de Castro, and T. Möller, <i>J. Phys. B</i> 41 , 181001 (2008).	451
427			452
428	[17] T. Katayama, S. Owada, T. Togashi, K. Ogawa, P. Karvinen <i>et al.</i> , <i>Struct. Dyn.</i> 3 , 034301 (2016).	[30] C. Bostedt, M. Adolph, E. Eremina, M. Hoener, D. Rupp, S. Schorb, H. Thomas, A. R. B. de Castro, and T. Möller, <i>J. Phys. B</i> 43 , 194011 (2010).	453
429			454
430	[18] T. Kameshima, S. Ono, T. Kudo, K. Ozaki, Y. Kiriwara <i>et al.</i> , <i>Rev. Sci. Instrum.</i> 85 , 033110 (2014).	[31] P. J. Ho, C. Knight, M. Tegze, G. Faigel, C. Bostedt, and L. Young, <i>Phys. Rev. A</i> 94 , 063823 (2016).	455
431			456
432	[19] H. Fukuzawa, K. Nagaya, and K. Ueda, <i>Nucl. Instrum. Methods Phys. Res., Sect. A</i> 907 , 116 (2018).		457
433			458
434	[20] D. R. Sears and H. P. Klug, <i>J. Chem. Phys.</i> 37 , 3002 (1962).		459
			460